A Novel Alphavirus Vaccine Encoding Prostate-Specific Membrane Antigen Elicits Potent Cellular and Humoral Immune Responses

Robert J. Durso,[1] Sofija Andjelic,[1] Jason P. Gardner,[1] Dennis J. Margitich,[1] Gerald P. Donovan,[1] Robert R. Arrigale,[1] Xinning Wang,[3] Maureen F. Maughan,[2] Todd L. Talarico,[2] Robert A. Olmsted,[2] Warren D.W. Heston,[3] Paul J. Maddon,[1] and William C. Olson[1]

Abstract

Purpose: Prostate-specific membrane antigen (PSMA) is an attractive target for active immunotherapy. Alphavirus vaccines have shown promise in eliciting immunity to tumor antigens. This study investigated the immunogenicity of alphavirus vaccine replicon particles (VRP) that encode PSMA (PSMA-VRP).

Experimental Design: Cells were infected with PSMA-VRP and evaluated for PSMA expression and folate hydrolase activity. Mice were immunized s.c. with PSMA-VRP or purified PSMA protein. Sera, splenocytes, and purified T cells were evaluated for the magnitude, durability, and epitope specificity of the anti-PSMA response. Antibodies were measured by flow cytometry, and cellular responses were measured by IFN-γ enzyme-linked immunospot and chromium release assays. Cellular responses in BALB/c and C57BL/6 mice were mapped using overlapping 15-mer PSMA peptides. A Good Laboratory Practice–compliant toxicology study was conducted in rabbits.

Results: PSMA-VRP directed high-level expression of active PSMA. Robust T-cell and B-cell responses were elicited by a single injection of 2×10^5 infectious units, and responses were boosted following repeat immunizations. Anti-PSMA responses were detected following three immunizations with 10^2 infectious units and increased with increasing dose. PSMA-VRP was more immunogenic than adjuvanted PSMA protein. Responses to PSMA-VRP were characterized by Th-1 cytokines, potent CTL activity, and IgG2a/IgG2b antibodies. T-cell responses in BALB/c and C57BL/6 mice were directed toward different PSMA peptides. Immunogenic doses of PSMA-VRP were well tolerated in mice and rabbits.

Conclusions: PSMA-VRP elicited potent cellular and humoral immunity in mice, and specific anti-PSMA responses were boosted on repeat dosing. PSMA-VRP represents a promising approach for immunotherapy of prostate cancer.

Prostate cancer is the most prevalent type of noncutaneous cancer in American men with an estimated 234,000 diagnosed cases and ~30,000 deaths in 2005 (1). Localized disease is generally treated with surgery or radiation therapy, and although recurrent or metastatic disease can be controlled temporarily with hormonal therapy, almost all prostate carcinomas eventually become androgen independent and then progress rapidly. Docetaxel in combination with prednisone is the only available nonpalliative therapy for androgen-independent prostate cancer. Treatment provides a modest survival benefit (2), and there is an urgent need for novel, molecularly targeted therapies. Metastatic prostate cancer is characterized by relatively small lesions within lymph node, bone marrow, and other sites within the immune system. These features may render prostate cancer more susceptible to vaccine immunotherapy than tumors that are characterized by bulkier or less accessible lesions.

Prostate-specific membrane antigen (PSMA) is the prototypic cell surface marker of prostate cancer. PSMA is an ~100-kDa type II integral membrane glycoprotein. In normal tissues, PSMA expression is largely limited to prostate. However, PSMA expression is up-regulated in prostate carcinomas (3, 4) and increases with disease progression, becoming highest in metastatic, hormone-refractory disease (5, 6). In addition, PSMA is abundantly expressed on the neovasculature of many other solid tumors but not on normal neovasculature (7–11). For these reasons, PSMA is considered to be an attractive target for cancer immunotherapy (reviewed in refs. 12, 13).

Alphaviruses are positive-strand RNA viruses that can mediate high-level gene expression in mammalian cells, and

Authors' Affiliations: [1]Progenics Pharmaceuticals, Inc., Tarrytown, New York; [2]AlphaVax, Inc., Research Triangle Park, North Carolina; and [3]Department of Cancer Biology, Cleveland Clinic Foundation, Cleveland, Ohio

Received 9/1/06; revised 3/22/07; accepted 3/30/07.

Grant support: NIH grants CA95928 and CA91746.

The costs of publication of this article were defrayed in part by the payment of page charges. This article must therefore be hereby marked *advertisement* in accordance with 18 U.S.C. Section 1734 solely to indicate this fact.

Note: Current address for J.P. Gardner: GlaxoSmithKline R&D, B38 2 58, Greenford Road, London UB6 0HE, United Kingdom.

Requests for reprints: William C. Olson, Progenics Pharmaceuticals, Inc., 777 Old Saw Mill River Road, Tarrytown, NY 10591. Phone: 914-789-2800; Fax: 914-789-2807; E-mail: olson@progenics.com.

doi:10.1158/1078-0432.CCR-06-2202

members of this family have served as a basis for viral vector and DNA plasmid vaccines for infectious diseases and cancer (reviewed in ref. 14). Recent preclinical studies have shown potent immunogenicity and antitumor effects for alphavirus vaccines encoding self-antigens (15–17). A propagation-defective vaccine replicon particle (VRP) vector system has been developed based on an attenuated variant of Venezuelan equine encephalitis virus (18, 19). Using tyrosinase as a prototypical melanocyte differentiation antigen, we recently showed that Venezuelan equine encephalitis virus–based VRP induced robust B-cell and T-cell responses and improved survival in mice challenged with B16 melanoma cells. In this setting, more potent and protective responses were elicited using a syngeneic (murine) rather than a xenogeneic (human) form of tyrosinase (17). Based on these findings, we prepared VRP encoding human PSMA for preclinical evaluation as a potential vaccine therapy for prostate cancer in man.

In the present study, we show that PSMA-VRP mediate high-level expression of native, enzymatically active, cell surface PSMA *in vitro* and potently elicit Th-1–biased cellular and humoral immunity to PSMA *in vivo*. Anti-PSMA responses were induced following a single injection of PSMA-VRP, and these responses were boosted on repeated dosing. The cellular immune responses in BALB/c and C57BL/6 mice were determined to be directed toward different defined peptide sequences within PSMA. Anti-PSMA immunity was elicited with a favorable safety profile both in mice and in a rabbit toxicology study that was conducted in compliance with Good Laboratory Practice regulations.

Materials and Methods

Cell lines. BHK-21 [Syrian hamster kidney fibroblast (20)] and Vero [African green monkey kidney (21)] cell lines were obtained from the American Type Culture Collection. Dr. Michelle Sadelain (Memorial Sloan-Kettering Cancer Center, New York, NY) generously provided CT26 cells (22) transduced with PSMA-encoding and empty retroviral vectors (CT26-PSMA and CT26-vector cells). CT26 is a murine colon adenocarcinoma that is syngeneic to BALB/c mice. 3T3-PSMA cells, parental 3T3 cells (23), and C4-2 cells (24), an androgen-independent subclone of the LNCaP prostate cancer cell line, have been described previously. All cell lines, except for C4-2 cells, were cultured in DMEM (Invitrogen) containing 10% heat-inactivated fetal bovine serum (Hyclone), 1 mmol/L sodium pyruvate, 100 μmol/L MEM nonessential amino acids, and 2 mmol/L GlutaMAX Supplement (all from Invitrogen). C4-2 cells were grown in RPMI 1640 (Invitrogen) containing the same supplements as listed for DMEM.

Generation of VRP. VRPs were generated as described previously (18). Briefly, the genes for human PSMA or green fluorescent protein (GFP) were directionally cloned into the replicon expression vector (phosphorylated extracellular signal-regulated kinase) and fully sequenced to verify authenticity. Full-length PSMA and GFP replicon RNA transcripts were generated *in vitro* using the RiboMax RNA Transcription kit (Promega). For VRP production, PSMA or GFP replicon RNA transcripts were mixed with two helper RNA transcripts encoding the Venezuelan equine encephalitis virus envelope and capsid proteins and then coelectroporated into BHK-21 or Vero cells in PBS using a GenePulser II electroporator (Bio-Rad). Following the incubation of cells for 16 to 24 h at 37°C, PSMA-VRP or GFP-VRP were harvested from the culture supernatant, purified by heparin chromatography, and stored at -80°C. To determine the infectious titers of the VRP preparations, expressed in infectious units (IU) per mL, Vero cells were infected with serial dilutions of PSMA-VRP or GFP-VRP for 1 h, washed, and incubated overnight. GFP expression was detected by fluorescence microscopy, whereas PSMA expression was measured using PSMA monoclonal antibody (mAb) CYT-351 (Cytogen) as a primary detection reagent followed by detection with FITC-conjugated anti-mouse antibody (Caltag).

PSMA peptides and PSMA$_{ECTO}$. The deduced protein sequence of full-length human PSMA (Genbank accession no. AF007544) was spanned using 15-mer peptides that overlapped by 10 amino acids (SynPep). Peptides were synthesized to >90% purity and identity tested by mass spectroscopy. Three peptides (LCAGALVLAGGFFLL, GFFLLGFLFGWFIKS, and IHSTNEVTRIYNVIG) could not be purified to >90% and were pooled separately (Pool-11). Six additional peptides (LVLAGGFFLLGFLFG, NFTQIPHLAGTEQNF, NYISIINEDGNEIFN, DMKINCSGKIVIARY, VKNFTEIASKFSERL, and QIYVAAFTVQAAAET) could not be successfully synthesized and were excluded from analysis. Individual peptides were pooled into nonoverlapping pools and lyophilized as described previously (25). Pools contained 13 to 15 peptides, except for Pool-11. Peptide pools were solubilized in DMSO (Sigma) at 10 to 20 mg/mL total peptide, whereas individual peptides were resuspended at 5 to 10 mg/mL. Following reconstitution, individual peptides and pools were aliquoted and stored at -80°C before use. The same set of peptide pools was used throughout this study.

Purified, dimeric PSMA$_{ECTO}$ protein was produced as described previously (26). Briefly, the extracellular domain of PSMA (amino acids 44-750) was expressed in secreted form in stably transfected Chinese hamster ovary cells and purified to homogeneity by column chromatography. Purified PSMA$_{ECTO}$ was stored at -80°C before use.

Western blot. BHK-21 cells at >80% confluency were infected in a six-well dish with PSMA-VRP or GFP-VRP at a multiplicity of infection (MOI) of 1. After 18 h of incubation at 37°C, VRP-infected cells and LNCaP cells were lysed in radioimmunoprecipitation assay buffer [1 mmol/L EDTA, 1% NP40 (Sigma), 1% Triton X-100 (Sigma), protease inhibitor cocktail (Sigma) in Dulbecco's PBS (DPBS; Invitrogen)] and cell debris was removed by centrifugation. Aliquots of extracts were boiled for 5 min under reducing conditions and loaded onto 4% to 15% Tris-glycine gels (Bio-Rad). Gels were transferred to nitrocellulose using a Trans-Blot SD (Bio-Rad) for 45 min at 15 V. Blots were blocked for 1 h at room temperature in blocking buffer [5% nonfat dry milk in 10% SDS (Invitrogen), 0.1% Triton X-100 in DPBS]. Blots were incubated for 1 h in 1 μg/mL PSMA mAb 544 (Maine Biotechnology) in blocking buffer, quickly rinsed twice, and washed thrice for 10 min and then incubated for 1 h with secondary antibody (goat anti-mouse IgG-horseradish peroxidase; Pierce) at 1:5,000 in blocking buffer. Blots were rinsed twice and washed once for 45 min and once for 5 min in wash buffer (10% SDS, 0.1% Triton X-100 in DPBS). Blots were developed using Western Lightning Plus (Perkin-Elmer) and X-OMAT XB-1 film (Kodak).

Flow cytometry assay for PSMA expression by PSMA-VRP. BHK-21 cells at >80% confluency were infected with PSMA-VRP at a MOI of 0, 0.003, 0.03, 0.3, or 3.0. After 18 h at 37°C, cells were washed in DPBS, released with cell dissociation solution (Sigma), and washed once in staining buffer [0.25% bovine serum albumin (Sigma) in DPBS]. Following a 20-min incubation at 4°C in blocking buffer [10% heat-inactivated goat serum (Invitrogen) in staining buffer], samples were stained with 1 μg of PSMA mAb 3.9 (27) for 30 min at 4°C. Cells were washed and centrifuged once with 10 volumes of staining buffer at 4°C. FITC-conjugated anti-mouse IgG was added at 0.5 μg/sample in staining buffer for 20 min at 4°C. Samples were again washed and centrifuged in staining buffer and analyzed on a FACSCalibur flow cytometer (Becton Dickinson). Mean fluorescence intensities (MFI) were calculated using CellQuest Pro software (Becton Dickinson).

Immunohistochemistry of PSMA-VRP–infected cells. BHK-21 cells at >80% confluency were infected with PSMA-VRP at MOI of 0, 0.01, 0.1, or 1.0. After 18 h at 37°C, cells were washed in DPBS, released with cell

dissociation solution, embedded with OCT medium (Miles), and frozen at -80°C. Sections 5 to 7 μm thick were cut on a Mictron HM505E cryostat at -10°C to -25°C and thaw mounted onto slides. Slides were incubated in Morphosave solution (Ventana Medica) for 15 min after fixation in acetone. Slides were washed twice in PBS, incubated for 20 min with 0.3% H_2O_2 in PBS, and washed once with PBS. After incubation with mouse PSMA mAb 3.1 (26) or isotype control antibody at 5 μg/mL for 30 min, slides were washed in Tris buffer, incubated with horseradish peroxidase–conjugated goat anti-mouse secondary antibody (DAKO) for 30 min, washed in Tris, and incubated twice for 5 min in 3,3′-diaminobenzidine (Sigma). Slides were washed again in Tris, counterstained in hematoxylin, rinsed in water, and finally dehydrated through a graded series of alcohols to xylene before analysis by light microscopy through a 20× Nikon Plan Apo objective using a Nikon Optiphot-2 with an Olympus Q-Color 3 camera system.

Folate hydrolase assay. BHK-21 cells were infected in T-150 flasks with PSMA-VRP or GFP-VRP at MOI of 1. After 18 h at 37°C, cells were harvested as described above, washed twice with PBS, and stored at -80°C before analysis. Cells were thawed, suspended in 50 mmol/L Tris (pH 7.5; 10 mL per T-150 flask), and disrupted with a Dounce homogenizer. Cell debris was removed by centrifugation at 3,000 × *g* for 5 min at 4°C, and the supernatant was then centrifuged at 70,000 × *g* for 35 min at 4°C. The pellet was washed in Tris buffer and homogenized in 1% Triton X-100 in Tris buffer. Protein concentration was determined by bicinchoninic acid assay, and 20 μg were combined with 5 μmol methotrexate diglutamate (Schircks Laboratories) in Tris buffer for 1 h at 37°C. The reaction was stopped by addition of Na_2HPO_4, and the mixture was analyzed by reversed-phase high-performance liquid chromatography as described previously (28, 29).

Mouse immunizations. BALB/c and C57BL/6 mice (Charles River Laboratories) were immunized by s.c. injections of PSMA-VRP or GFP-VRP in a total volume of 20 μL into the plantar surface of the left hind footpad using a Microfine-IV insulin syringe (Becton Dickinson) every 2 weeks. Tolerability was assessed by monitoring the appearance and weight of immunized animals. BALB/c mice (five per group) were immunized with 10 μg $PSMA_{ECTO}$ adsorbed onto 250 μg Alhydrogel (alum, Brenntag Biosector) according to published methods (26). Vaccine was administered s.c. in the leg at weeks 0, 2, and 6. The 4-week rest period before the final immunization was selected based on our prior study of $PSMA_{ECTO}$/alum (26). Sera and splenocytes were collected for analysis 2 weeks after the final immunization.

Serology assays for PSMA antibodies. Blood was isolated from the mouse orbital sinus plexus using a nonheparinized glass capillary tube and collected into a CapiJect capillary blood collection tube (Terumo Medical Corp.) containing a gel/clot activator. Serum was isolated by centrifugation and stored at -20°C before analysis by flow cytometry and ELISA. For flow cytometry analyses, serum was diluted 1:100 in staining buffer and added to 2×10^5 3T3 or 3T3-PSMA cells in blocking buffer (10% heat-inactivated goat serum in staining buffer) for 30 min at 4°C. Cells were washed with 10 volumes of staining buffer at 4°C. Secondary FITC-conjugated anti-mouse IgG antibody was added for 20 min at 4°C. Samples were washed in staining buffer and analyzed by flow cytometry as described above.

For ELISA analyses, 3T3-PSMA cells were plated in Biocoat poly-L-lysine 96-well assay plates (BD Biosciences) overnight at 37°C. Wells were washed once with wash buffer (DPBS containing 5% fetal bovine serum) and blocked for 2 h at room temperature with DPBS containing 3% bovine serum albumin. Wells were decanted, and serum from immunized animals was added for 2 h at room temperature. Plates were washed thrice in wash buffer, and alkaline phosphatase–conjugated goat antibody to mouse IgG or mouse IgG subtypes (Caltag) was added at 1:1,000 dilution for 1 h at room temperature. Plates were washed thrice in wash buffer, developed for 1 h at 25°C with pNPP/DEA substrate (Pierce), and read on a SpectraMax 340 plate reader at wavelengths of 405 and 650 nm. End point titer was defined as the highest dilution of the immune serum yielding an absorbance of 0.100 above background.

Isolation of T lymphocytes. Spleens were harvested from immunized animals, and splenocytes were isolated by manual disruption of the spleen using aseptic technique. Single-cell suspensions were prepared by passage of cells through a 70-μm filter (BD Biosciences). Red cells were lysed using ACK lysing buffer (Cambrex) following the manufacturer's instructions, and splenocytes were resuspended into T-cell medium (RPMI 1640/MEM, α-medium 1:1 with 10% heat-inactivated fetal bovine serum, 10 mmol/L HEPES, 1 mmol/L sodium pyruvate, 100 μmol/L MEM nonessential amino acids, 2 mmol/L GlutaMAX Supplement, and 55 nmol/L 2-mercaptoethanol, all from Invitrogen). $CD8^+$ T lymphocytes were isolated from bulk splenocytes by positive selection using anti-mouse CD8a (Ly-2) microbeads, whereas $CD4^+$ T lymphocytes were isolated by positive selection with anti-mouse CD4 microbeads (Miltenyi Biotec) according to the manufacturer's guidelines. Purity of the isolated subsets was analyzed by flow cytometry and typically was >95%.

Enzyme-linked immunospot assay. Multiscreen nitrocellulose or Multiscreen HTS IP enzyme-linked immunospot (ELISPOT) plates (Millipore) were coated overnight at 4°C with 1 μg/well anti-mouse IFN-γ mAb (clone AN18; Mabtech) and blocked for 2 h at 37°C in T-cell medium (see above). Splenocytes (3×10^5 per well) were allowed to settle onto the membrane for 30 min at 37°C. CT26-vector or CT26-PSMA cells ($H\text{-}2^d$ positive, BALB/c syngeneic stimulator cells) were pretreated for 30 min at 37°C with 100 μg/mL mitomycin C (Sigma), washed, and allowed to recover for 1 h at 37°C before addition at 2×10^5 per well. As controls, either medium alone or phorbol 12-myristate 13-acetate and calcium ionomycin (Sigma) were added at final concentrations of 1 and 0.5 μg/mL, respectively. Following 18 h of incubation at 37°C, cells were decanted and plates were washed six times with wash buffer [0.05% Tween 20 (Sigma) in DPBS without Ca/Mg ($DPBS^-$; Invitrogen)]. Biotinylated anti-mouse IFN-γ mAb (clone R4-6A2; Mabtech) was added at 0.4 μg/mL in 0.5% bovine serum albumin in $DPBS^-$ to each well and the plates were incubated for 2 h at 37°C. After washing the plates six times in wash buffer, 100 μL of enzyme complex (Vectastain Standard Elite avidin-biotin complex kit, Vector Laboratories) were added for 1 h at ambient temperature. Plates were washed thrice in wash buffer and thrice in PBS. Excess liquid was removed, and wells were developed for 4 min at room temperature with 3-amino-9-ethylcarbazole (Vector Laboratories). The substrate was decanted and the plates were washed with water before drying. Membranes were transferred to sealing tape (Millipore) and spots were counted on a KS ELISPOT System (Carl Zeiss). For the anti-interleukin-4 (IL-4) ELISPOT, plates were coated with anti-mouse IL-4 mAb (clone 11B11; Mabtech) and developed using biotinylated anti-mouse IL-4 mAb (clone BVD6-24G2; Mabtech) after a 40-h incubation at 37°C. Background was defined as the number of IFN-γ or IL-4 spot-forming cells (SFC) per number of cells plated in the presence of medium only (in all cases, background SFCs per 3×10^5 cells were <10). A positive response was defined as greater than 3 SDs above the mean background signal.

For peptide-based ELISPOT assays, bulk splenocytes from immunized animals were plated at 3×10^5 per well in IFN-γ-coated ELISPOT plates as described above. Alternatively, $CD8^+$ or $CD4^+$ T cells were isolated as described above and mixed in a 2:1 ratio with CD8/CD4-depleted splenocytes from nonimmunized mice to generate 3×10^5 per well. Data are reported as SFCs per 3×10^5 $CD8^+$ or $CD4^+$ cells for consistency. Cells were stimulated with individual or pooled PSMA peptides or pooled HIV gag peptides (p55, BD Biosciences) at a concentration of 2 μg/mL of each individual peptide, and the ELISPOT assay was developed as described above.

Dendritic cells were used as stimulators in some ELISPOT assays. Briefly, bone marrow cells were isolated from the tibia and femurs of naive BALB/c mice, and mononuclear cells were isolated using Lympholyte-M (Cederlane Laboratories) according to the manufacturer's instructions. Cells were grown in T-cell medium (see above)

supplemented with 1,000 units/mL of mouse granulocyte macrophage colony-stimulating factor (GM-CSF) and mouse IL-4. Cells were cultured for 8 days in the presence of GM-CSF/IL-4 or for 6 days with GM-CSF/IL-4 followed by 2 days with GM-CSF/IL-4 plus 250 ng/mL murine tumor necrosis factor-α. Fresh cytokine-containing medium was added every other day during culture. Cytokines were purchased from R&D Systems. Cells were analyzed by flow cytometry for dendritic cell markers and infected at MOI of 5 with PSMA-VRP and GFP-VRP or left uninfected. After 18 h at 37°C, cells were washed and combined with 3×10^5 splenocytes, and ELISPOT plates were processed as described above.

CTL assay. Splenocytes were isolated from immunized BALB/c mice as described above and incubated at 5×10^6 cells/mL with PSMA peptide 16 (NFTQIPHLAGTEQNF) at 10 μg/mL for 5 days. CT26-PSMA or CT26-vector target cells were labeled with 250 μCi of $Na_2^{51}CrO_4$ for 1 h and washed. Target cells and splenocyte effector cells were combined for 4 h in duplicate wells of a 96-well round-bottomed plate. Plates were centrifuged, and supernatants were harvested using a Skatron Supernatant Collection System (Molecular Devices). Specific lysis was determined following γ-counting (Perkin-Elmer) using the following formula: % specific lysis = 100 × (test release in the presence of effector cells - spontaneous release) / (maximal release - spontaneous release). Spontaneous release was determined based on wells containing labeled target cells only, whereas maximum release was determined by lysing labeled target cells with 1 N HCl.

Rabbit toxicology study. A Good Laboratory Practice–compliant toxicology study was done in male New Zealand White rabbits. Animals ($n = 6$) were inoculated s.c. with four doses of 2×10^7 IU or 2×10^8 IU of PSMA-VRP. A negative control group received vehicle only. Animals were immunized at 2-week intervals, and half of the animals were sacrificed for histopathology either 2 days or 2 weeks after the final injection. Systemic toxicity was evaluated by recording mortality/morbidity, body temperature, body weight, food consumption, and ophthalmic examinations. Hematopoietic toxicity was evaluated by quantitating cellular components of peripheral blood. Potential immune system and autoimmune toxicities were assessed by histopathologic examination of lymphoid organs, prostate, brain, duodenum, kidneys, and other tissues. Organ toxicity also was assessed by monitoring clinical chemistry variables. Local reactogenicity was evaluated by examining injection sites both grossly and microscopically. Preimmune and postimmune sera were tested at a 1:200 dilution for binding to 3T3-PSMA cells by flow cytometry as described above.

Results

PSMA-VRP mediates high-level expression of enzymatically active PSMA. To examine the expression of PSMA by PSMA-VRP *in vitro*, BHK-21 cells were infected with PSMA-VRP or GFP-VRP (control VRP) at a MOI of 1. Whole-cell lysates were analyzed for PSMA expression by Western blotting (Fig. 1A). A single band of ~100 kDa was identified in cells infected with PSMA-VRP, but not GFP-VRP, and this band comigrated with PSMA expressed in LNCaP cells, suggesting that PSMA-VRP directs expression of full-length PSMA with a normal extent of glycosylation.

BHK-21 cells were infected with PSMA-VRP and further analyzed by flow cytometry with a conformation-dependent anti-PSMA mAb (26). PSMA was detected at the surface of infected cells, and expression levels increased with increasing MOI ranging from 0.003 to 3.0 (Fig. 1B). No PSMA expression was detected in uninfected cells (Fig. 1B) or in cells infected with GFP-VRP (data not shown). In addition, immunohistochemistry was used to examine PSMA expression in BHK-21 cells infected with PSMA-VRP at MOI of 0.01, 0.1, and 1.0 (Fig. 1C). Consistent with the flow cytometry data, PSMA expression increased as the MOI was increased from over this range, and no staining was observed for uninfected cells (Fig. 1C) or for cells stained with isotype control antibody (data not shown). At the highest MOI (1.0), PSMA expression was comparable with or greater than that on PSMA-3T3 cells (data not shown), which express PSMA at $>10^6$ copies/cell (30). These studies show that PSMA-VRP directs high-level surface expression of native PSMA in mammalian cells *in vitro*.

BHK-21 cells were evaluated for folate hydrolase activity following infection with PSMA-VRP. Uninfected cells and cells infected with GFP-VRP served as controls. Consistent, high-level enzyme activity was observed in cells infected with PSMA-VRP (Fig. 1D). The level of activity (~50 nmol glutamate released/mg protein/h) in infected BHK-21 cells was comparable with that observed in C4.2 cells, an androgen-independent prostate cancer cell line with high endogenous expression of PSMA (29). In contrast, no significant activity was observed for uninfected cells or cells infected with GFP-VRP. The findings indicate that PSMA-VRP induces expression of enzymatically active PSMA.

PSMA-VRP induces potent, Th-1–biased humoral and cellular immune responses. BALB/c mice were vaccinated with either a single s.c. injection or repeated biweekly s.c. injections of PSMA-VRP, and serum was collected for analysis of the humoral response by flow cytometry and ELISA. A single injection with 2×10^5 IU PSMA-VRP induced a significant anti-PSMA IgG response as measured by flow cytometry against 3T3-PSMA cells, whereas repeated immunizations substantially augmented the PSMA antibody response (Fig. 2A). In a second set of immunizations in BALB/c mice ($n = 5$/group), three doses of 2×10^5 IU PSMA-VRP were compared directly with three doses of 10 μg $PSMA_{ECTO}$/alum, and sera were analyzed in parallel by flow cytometry. In this experiment, PSMA-VRP induced significantly ($P = 0.012$, two-sided t test) higher levels of anti-PSMA antibodies (MFI = 148 ± 29) than did $PSMA_{ECTO}$/alum (MFI = 94 ± 23).

As measured by ELISA, mean PSMA antibody end point titers increased from 1:200 following a single 2×10^5 IU dose to 1:3,200 following three doses of 2×10^5 IU PSMA-VRP (data not shown). We next used the PSMA-specific ELISA to characterize the isotype distribution of the anti-PSMA IgG antibodies induced by immunization with PSMA-VRP. The predominant isotypes were identified to be IgG2a and IgG2b (Fig. 2B). IgG2a was detected with 7-fold greater efficiency than IgG1, and this distribution is reflective of a Th-1 response.

Splenocytes from PSMA-VRP–vaccinated mice were analyzed by an IFN-γ ELISPOT assay to assess the induction of the cellular immune response to PSMA. Bulk splenocytes from immunized BALB/c mice were stimulated with syngeneic CT26-PSMA or CT26-vector cells. A significant PSMA-specific IFN-γ secretion (95 ± 33 SFCs per 3×10^5 splenocytes) was observed from splenic T cells after a single 2×10^5 IU immunization, and this response was increased 5-fold (456 ± 90 SFCs per 3×10^5 splenocytes) following three biweekly s.c. vaccinations (Fig. 2C). In contrast, background levels of SFC were observed following three immunizations with GFP-VRP or using CT26-vector cells for stimulation (Fig. 2C). Significant anti-PSMA B-cell and T-cell responses were observed even 1 year after the final immunization (data not shown), indicating that the immunity is long lived.

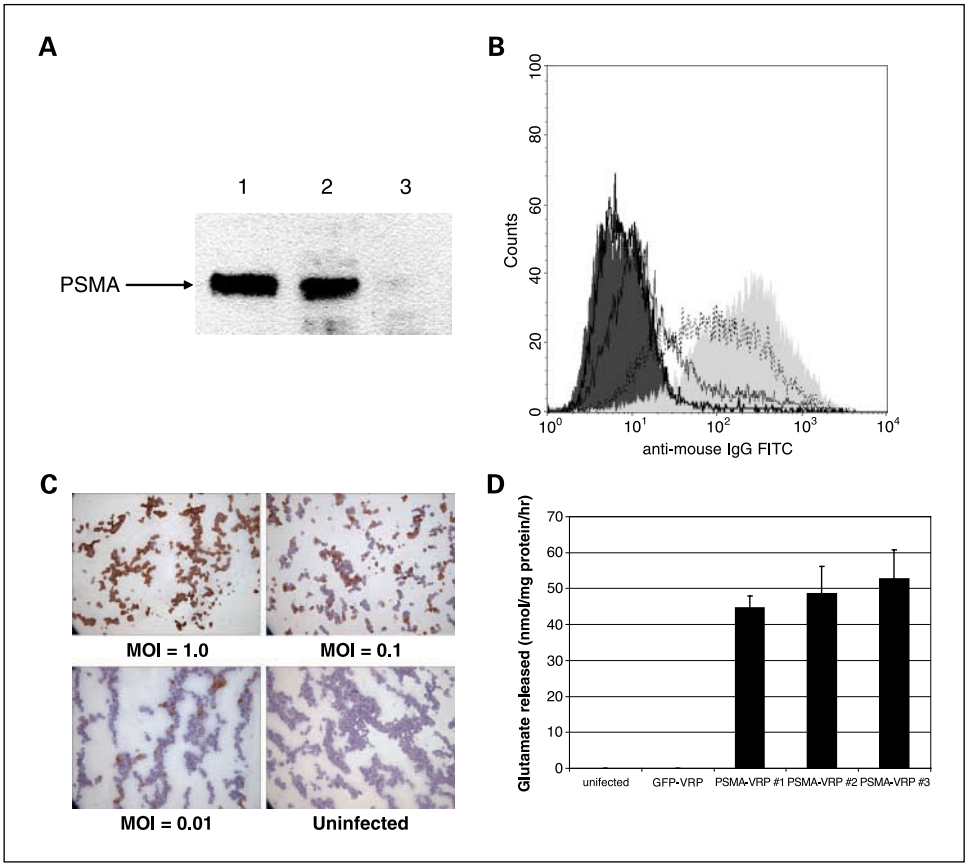

Fig. 1. PSMA-VRP directs high-level expression of native, cell surface PSMA. *A*, Western blot analysis of PSMA expression. BHK-21 cells were infected with PSMA-VRP or GFP-VRP at a MOI of 1. LNCaP cells (*lane 1*) and BHK-21 cells infected with PSMA-VRP (*lane 2*) or GFP-VRP (*lane 3*) were analyzed by Western blotting using PSMA mAb 544. *B,* BHK-21 cells were infected with PSMA-VRP and analyzed for PSMA expression by flow cytometry using PSMA mAb 3.9. Histogram overlays show MOIs of 3 (*light shading*), 0.3 (*dotted line*), 0.03 (*thin line*), 0.003 (*heavy line*), or uninfected cells (*dark shading*). *C,* immunohistochemistry of BHK-21 cells infected with PSMA-VRP at the indicated MOI. Sections were stained with PSMA mAb 3.1, and images were obtained at ×20 magnification. *D,* membrane fractions from infected and uninfected BHK-21 cells were analyzed for folate hydrolase activity. Cells were infected with PSMA-VRP or GFP-VRP at MOI of 1. PSMA-VRP membranes were prepared from each of three separate infections in T-150 flasks, and each membrane preparation was analyzed in triplicate. Columns, mean of triplicate reactions; bars, SD.

In contrast to the robust PSMA-specific IFN-δ responses elicited by PSMA-VRP (Fig. 2C), no significant IL-4 secretion was observed by ELISPOT following stimulation of cells with CT26-PSMA (data not shown). This Th-1 cytokine profile is consistent with the Th-1 bias of the antibody response (Fig. 2B). In addition, no PSMA-specific IFN-γ response was observed for bulk splenocytes from animals immunized with three doses of $PSMA_{ECTO}$/alum (<2 SFCs per 3×10^5 cells).

Dose dependency of the immune response elicited by PSMA-VRP. PSMA-specific cellular and humoral immune responses were evaluated in BALB/c mice following three biweekly s.c. injections of PSMA-VRP at dose levels of 10^2, 10^4, and 10^6 IU. Control animals received three injections of 10^6 IU GFP-VRP. A 10^2 IU dose of PSMA-VRP induced measurable levels of PSMA antibodies in three of five mice, whereas all animals seroconverted at the two higher dose levels. The MFI values were 16 ± 11, 68 ± 31, and 112 ± 14 for animals immunized with 10^2, 10^4, and 10^6 IU PSMA-VRP, respectively, whereas MFI values were 6 ± 1 for animals immunized with 10^6 IU GFP-VRP (Fig. 2D).

Splenic $CD8^+$ T cells were isolated from these animals and tested for IFN-γ secretion by ELISPOT assay using CT26-PSMA or CT26-vector cells for stimulation. Compared with the humoral response, the cellular response to PSMA-VRP was similarly dose dependent (Fig. 2E). At a dose of 10^2 IU PSMA-VRP, the number of SFC (13 ± 3 per 3×10^5 cells) was marginally but not significantly higher than that observed for animals immunized with 10^6 IU GFP-VRP. However, a 10^4 IU dose elicited significant PSMA-specific IFN-γ secretion (162 ± 13 SFCs per 3×10^5 cells), and this response was 4-fold higher at 10^6 IU (662 ± 65 SFCs per 3×10^5 cells; Fig. 2D). The weight and appearance of animals were monitored at least twice weekly, and no sign of toxicity was observed by these measures.

PSMA-VRP elicits a functional CTL response. We next used a chromium release assay to examine the CTL activity elicited by PSMA-VRP. Splenocytes from BALB/c mice immunized with PSMA-VRP or vehicle were used as effectors, and syngeneic CT26-PSMA and CT26-vector control cells were used as targets. Potent CTL activity was observed for PSMA-VRP splenocytes, which lysed up to 60% to 70% of CD26-PSMA targets (Fig. 2F). Cell killing was PSMA specific, as <5% cell lysis was observed for PSMA-VRP splenocytes tested against CT26-vector controls or for splenocytes from vehicle-immunized animals tested against either CT26-PSMA or CT26-vector cells (Fig. 2F).

Mapping the anti-PSMA cellular immune response in BALB/c and C57BL/6 mice. To dissect the epitope specificity of the immune response induced by PSMA-VRP, peptides spanning the entire amino acid sequence of human PSMA were used to stimulate lymphocytes from immunized mice in an IFN-γ ELISPOT assay. IFN-γ ELISPOT data obtained on total splenocytes from PSMA-VRP immunized BALB/c mice identified a single peptide pool (PSMA Pool-6) that is responsible for the immune reactivity in this assay (Fig. 3A). The IFN-γ response directed to Pool-6 (115 ± 39 SFCs per 3×10^5 cells) was similar in magnitude to that directed against CT26-PSMA stimulator cells (151 ± 20 SFCs per 3×10^5 cells). In contrast, no significant IFN-γ responses were observed for splenocytes from animals immunized with $PSMA_{ECTO}$/alum (≤4 SFCs per 3×10^5 cells for all peptide pools).

Bulk splenocytes and purified $CD8^+$ T cells were next tested against the individual peptides that comprise Pool-6 (Fig. 3B).

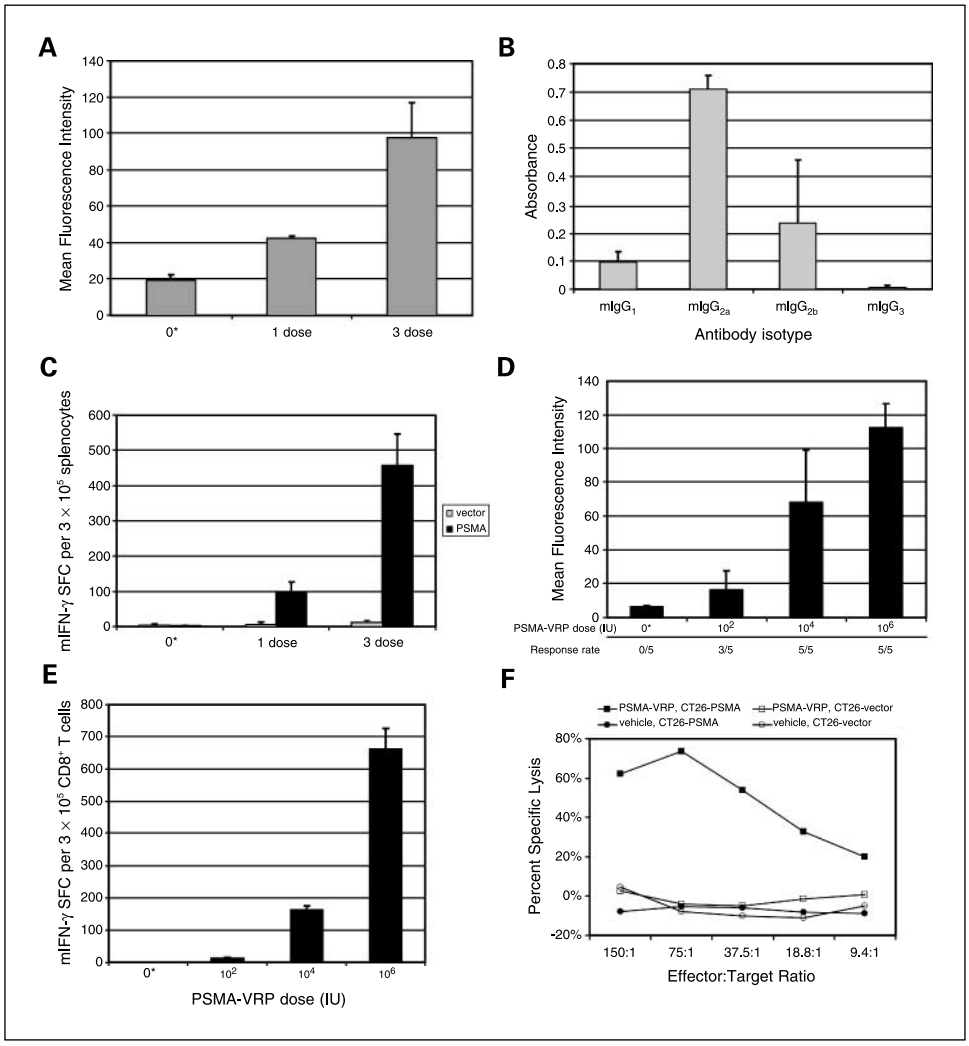

Fig. 2. Single and repeat administration of PSMA-VRP vaccine induces potent, dose-dependent humoral and cellular immunity. *A,* BALB/c mice (five per group) were immunized once or thrice at biweekly intervals with 2×10^5 IU PSMA-VRP or thrice with 2×10^5 IU control GFP-VRP (*0**). Immune sera were collected 2 wks after the final immunization and tested at 1:100 dilution for reactivity with 3T3-PSMA or parental control 3T3 cells by flow cytometry. MFI values for serum binding to parental 3T3 cells were 17.9 ± 3.5. *B,* isotype distribution of anti-PSMA antibodies elicited by PSMA-VRP. BALB/c mice ($n = 5$) were immunized with 2×10^5 IU PSMA-VRP thrice biweekly, and serum was collected 2 wks after the third dose and tested at 1:100 dilution in a PSMA-specific ELISA assay using isotype-specific reporter antibodies for detection. Columns, mean of triplicate values. *C,* spleens were isolated from animals immunized in (*A*), and splenocytes were analyzed by IFN-γ ELISPOT assay using CT26-PSMA cells (*PSMA, darker shading*) or CT26-vector control cells (*vector, lighter shading*) for stimulation. Columns, mean of triplicate values of SFCs; bars, SD. *D,* PSMA-specific antibody response was analyzed 2 wks after three biweekly injections of either 10^2, 10^4, or 10^6 IU PSMA-VRP or 10^6 IU GFP-VRP (*0**) in BALB/c mice (five per group). Samples were tested by flow cytometry as described above. The data are representative of two experiments. *E,* IFN-γ ELISPOT of purified $CD8^+$ T cells from spleens of animals in (*C*). Columns, mean of triplicate values; bars, SD. *F,* CTL activity. BALB/c mice ($n = 5$) were immunized thrice biweekly with 2×10^5 IU PSMA-VRP or formulation vehicle. Splenocytes were collected 2 wks after the last immunization, stimulated for 5 d with PSMA peptide (NFTQIPHLAGTEQNF), and tested for the ability to lyse CT26-PSMA or CT26-vector control cells that had been labeled with $Na_2^{51}CrO_4$. Points, mean of two independent assays.

In this assay, a potent immune response (416 ± 33 SFCs per 3×10^5 $CD8^+$ T cells) was observed against a single 15-mer peptide, Peptide 16 ($PSMA_{76\text{-}90}$, NFTQIPHLAGTEQNF). The splenocyte response to Peptide 16 was similar in magnitude to that observed for Pool-6 (384 ± 12 SFCs per 3×10^5 splenocytes), and no significant response was observed to the other peptides within Pool-6. The findings from the peptide-based IFN-γ ELISPOT assays indicate that the $CD8^+$ T-cell response is targeted to an immunodominant determinant in Peptide 16.

Purified $CD4^+$ T cells also readily responded to Peptide 16, albeit at a substantially lower level (51 ± 12 SFCs per 3×10^5 $CD4^+$ T cells; Fig. 3C), indicating that this peptide may contain a MHC class II determinant. The purity of isolated $CD8^+$ and $CD4^+$ T-cell subsets was typically >95% as determined by flow cytometry analysis (data not shown); however, we cannot exclude the possibility that the response observed in the $CD4^+$ T-cell population against Peptide 16 was due to low-level presence of PSMA-specific $CD8^+$ T cells. In addition, $CD4^+$ T cells also showed a weak response (17 ± 5 SFCs per 3×10^5 $CD4^+$ T cells) against Peptide 146 (also a component of Pool-6; Fig. 3C). The sequence for Peptide 146, $PSMA_{726\text{-}740}$ (GEVKRQIYVAAFTVQ), partially corresponds to one previously predicted to bind to human HLA-DR class II (31).

We next examined whether dendritic cells could be transduced by PSMA-VRP *in vitro* and used to stimulate T cells from immunized animals. Dendritic cells from naive BALB/c mice were matured from bone marrow cells *in vitro*, infected with PSMA-VRP or GFP-VRP, and combined with splenocytes from mice immunized with PSMA-VRP or vehicle in an IFN-γ ELISPOT assay. Dendritic cells transduced with PSMA-VRP *in vitro* efficiently stimulated splenocytes from animals immunized with PSMA-VRP but not animals immunized with vehicle (Fig. 3D). Dendritic cells that were matured using GM-CSF plus IL-4 alone were more effective stimulators (82 ± 16 SFCs per 3×10^5 splenocytes) than dendritic cells matured using GM-CSF, IL-4, and tumor necrosis factor-α (43 ± 8 SFCs per 3×10^5 splenocytes). Regardless of the method of dendritic cell maturation, the number of SFC observed following transduction with PSMA-VRP was significantly greater ($P < 0.02$, two-sided t test) than that observed either with cells transduced with GFP-VRP or with uninfected cells (Fig. 3D).

A second mouse strain, C57BL/6, was vaccinated to determine if the breadth and potency of PSMA-VRP–induced immune response are MHC haplotype dependent. Similar to data obtained in BALB/c mice, 2×10^5 IU PSMA-VRP elicited high levels of PSMA antibodies in C57BL/6 mice (123 ± 31 MFI; data not shown) and a vigorous cellular response in the

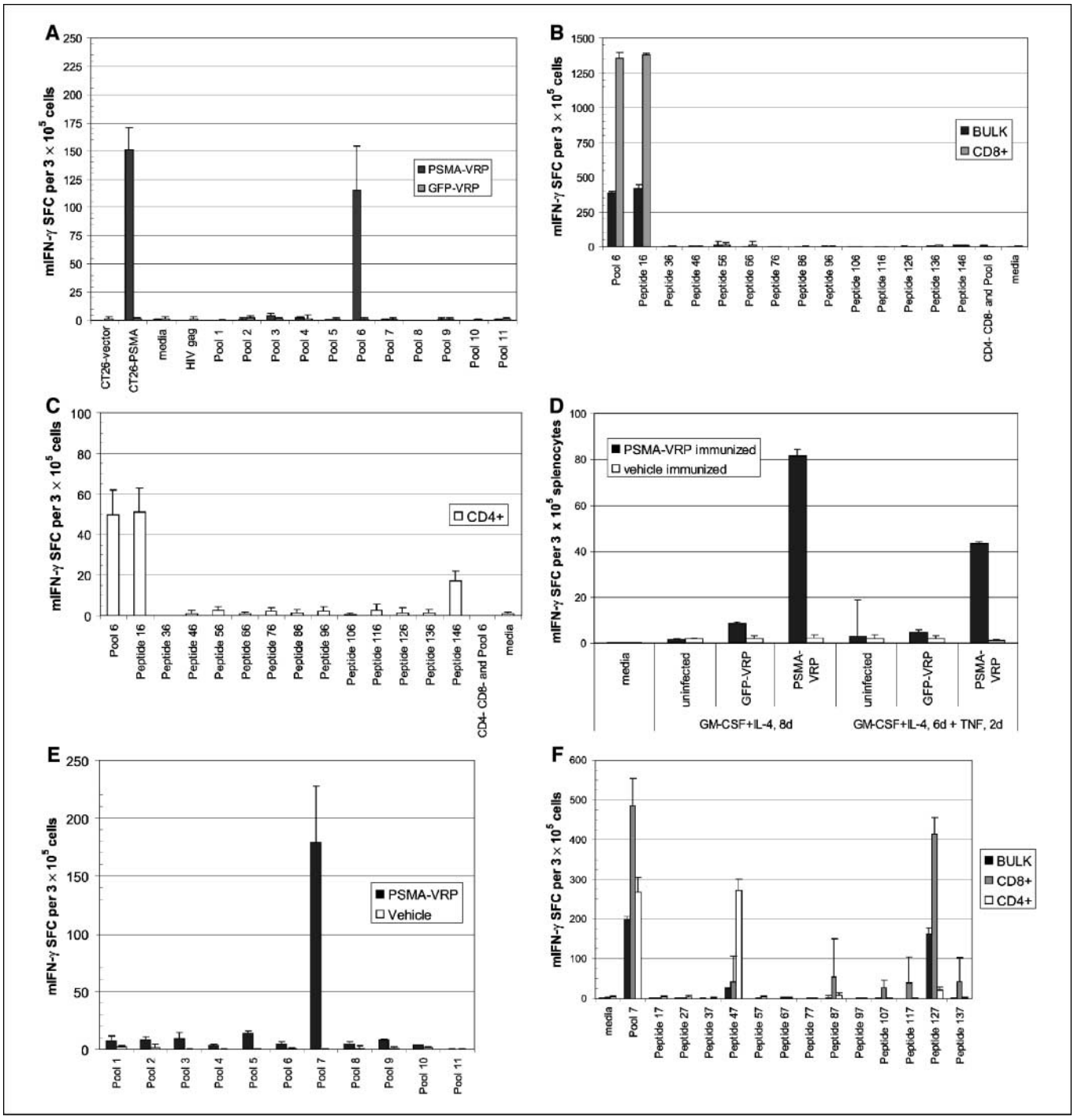

Fig. 3. Epitope specificity of the T-cell response elicited by PSMA-VRP. *A,* PSMA-specific immune responses were analyzed 2 wks after a thrice-biweekly regimen in BALB/c mice with PSMA-VRP or GFP-VRP. Bulk splenocytes (3×10^5) were plated onto an anti – IFN-γ-coated ELISPOT plate with CT26-vector or CT26-PSMA cells, mitogen, medium, or HIV gag (control) or PSMA peptide pools containing 2 μg/mL of each individual peptide. Columns, mean SFCs from triplicates; bars, SD. *B* and *C,* 2×10^5 $CD8^+$ or $CD4^+$ splenic T cells from mice in (*A*) were isolated using Miltenyi MACS columns and plated with 1×10^5 $CD4^-CD8^-$ cells isolated from nonimmunized mice (in a 2:1 ratio) onto an anti – IFN-γ-coated ELISPOT plate. Cells were stimulated with CT26-vector or CT26-PSMA cells, mitogen, medium, or 2 μg/mL of peptides as indicated. Data are the number of SFCs per number of $CD4^+$ or $CD8^+$ cells. Columns, mean of triplicate wells; bars, SD. *D,* IFN-γ responses observed using transduced dendritic cells for stimulation. Dendritic cells from naive mice were matured using GM-CSF and IL-4 or using GM-CSF, IL-4, and tumor necrosis factor-α as indicated. Uninfected dendritic cells or dendritic cells infected *in vitro* with PSMA-VRP or GFP-VRP were used in an IFN-γ ELISPOT assay to stimulate splenocytes from BALB/c mice that had been immunized thrice biweekly with 2×10^5 IU PSMA-VRP vehicle. Splenocytes were stimulated in parallel with PSMA Peptide 16 (NFTQIPHLAGTEQNF), and responses of 554 ± 24 SFCs per 3×10^5 cells and <1 SFCs per 3×10^5 splenocytes were observed for PSMA-VRP and vehicle animals, respectively. Columns, mean of triplicate analyses; bars, SD. *E,* C57BL/6 mice were immunized (thrice biweekly) with 2×10^5 IU PSMA-VRP (*black columns*) or vehicle (*white columns*), and spleens were isolated 2 wks after the final injection. Bulk splenocytes were analyzed by ELISPOT for IFN-γ secretion following stimulation with blank medium or PSMA peptide pools. Columns, mean triplicate values of SFCs; bars, SD. *F,* 2×10^5 $CD8^+$ or $CD4^+$ splenic T cells from PSMA-VRP mice of (*E*) were isolated using Miltenyi MACS columns and plated with 1×10^5 $CD4^-CD8^-$ cells isolated from nonimmunized C57BL/6 mice (in a 2:1 ratio) onto an IFN-γ-coated ELISPOT plate. Cells were stimulated with conditions listed above. Dark shading, bulk splenocytes; light shading, $CD8^+$ T cells; no shading, $CD4^+$ T cells. Data are the number of SFCs per number of $CD4^+$ or $CD8^+$ cells. Columns, mean of triplicate wells; bars, SD. Assay background for all samples in (*A*) to (*F*) was $\leq 3 \pm 2$ SFCs per 3×10^5 cells.

peptide-based ELISPOT assay (178 ± 49 SFCs per 3×10^5 splenocytes; Fig. 3E). However, the cellular response in C57BL/6 mice was focused toward a different PSMA peptide pool (Pool-7; Fig. 3E). In addition, responses of lower magnitude (<20 SFCs per 3×10^5 splenocytes) were observed for other pools (1, 2, 3, 5, and 9) in C57BL/6 mice, indicating additional reactivities. Notably, the C57BL/6 splenocytes did not respond to Pool-6 (Fig. 3E), which was the focus of the response elicited by PSMA-VRP in BALB/c animals (Fig. 3A). The nonoverlapping determinants of IFN-γ responses in C57BL/6 mice (primarily Pool-7) and BALB/c mice (primarily Pool-6) provide additional specificity controls of our ELISPOT methods.

Using individual peptides from Pool-7, the major $CD8^+$ T-cell reactivity in C57BL/6 mice was mapped to Peptide 127 ($PSMA_{631-645}$, SLFSAVKNFTEIASK, 414 ± 42 SFCs per 3×10^5 $CD8^+$ cells; Fig. 3E), whereas $CD4^+$ T cells responded strongly to Peptide 47 ($PSMA_{231-245}$, PADYFAPGVKSYPDG, 181 ± 21 SFCs per 3×10^5 $CD4^+$ cells; Fig. 3E). $CD8^+$ T cells also displayed low but detectable responses (18-37 SFCs per 3×10^5 $CD8^+$ cells) against several other peptides within Pool-7 (Fig. 3F). These additional responses were not detected in bulk splenocytes, possibly due to the smaller proportion of responding cells in the unfractionated population.

Whereas the $CD4^+$ T cells in both BALB/c- and C57BL/6-vaccinated mice secreted IFN-γ on stimulation with PSMA peptides (Fig. 3), these cells did not secrete IL-4 in parallel ELISPOT assays (data not shown). However, these cells effectively secreted IL-4 when stimulated with mitogen (176 ± 34 per 2×10^5 cells). This result indicates that lack of IL-4 secretion following stimulation with PSMA peptides was not due to an IL-4 deficiency of $CD4^+$ T cells but rather reflects the Th-1 bias of the cellular response induced by PSMA-VRP.

Tolerability in rabbits. A Good Laboratory Practice–compliant toxicology study was conducted to examine the potential toxicity and immunogenicity of PSMA-VRP in male rabbits. Following four s.c. injections of 2×10^7 IU or 2×10^8 IU PSMA-VRP on a biweekly schedule, all animals survived to their scheduled sacrifice. There was no evidence of vaccine-related systemic, hematopoietic, immune, or other organ toxicity at any dose or time in the study. Prostate, brain, kidney, and small intestine were unaffected. Physical examination of the injection site showed minimal erythema that resolved within 1 to 2 days and was not related to PSMA-VRP. Anti-PSMA antibodies were observed in zero of six vehicle animals, five of six animals in the low-dose PSMA-VRP group, and six of six animals in the high-dose group. Therefore, immunogenic doses of PSMA-VRP were well tolerated in this study.

Discussion

The present study represents the first preclinical evaluation of a novel alphavirus vector vaccine for prostate cancer. PSMA-VRP mediated high-level expression of PSMA in mammalian cells *in vitro*. The antigen reached the cell surface, showed carboxypeptidase activity, and was recognized by a conformation-specific antibody. Potent, Th-1–biased antibody responses and CTL responses were observed in mice, and the epitope specificity of the cellular immune response was mapped to specific peptide sequences within PSMA. The product was immunogenic and well tolerated in a rabbit toxicology study. The findings support further evaluation of PSMA-VRP as a new immunotherapeutic approach to treat advanced prostate cancer and/or to prevent disease recurrence.

PSMA-VRP elicited robust anti-PSMA immune responses in each of two mouse strains and in rabbits. Therefore, the immunopotency of PSMA-VRP is not restricted to mice but rather is also seen in a larger, nonrodent species. A dose of 100 IU of PSMA-VRP was sufficient to elicit PSMA-specific B-cell and T-cell immunity in mice. The highest responses were observed at doses of 10^6 IU, and no overt toxicity was observed over this dose range in mice. Similarly, doses ranging to 2×10^8 IU were well tolerated in a rabbit toxicology study, and this information is relevant to the selection of doses for human testing.

The utility of viral-based vaccines often is limited by antivector immunity, and such vaccines typically are used as a booster injection following priming with DNA or other vaccine approaches (17, 32, 33). Consequently, there is limited potential for continued immune stimulation following the booster injection. In the present study, PSMA-VRP was used without a heterologous prime, and repeat dosing with PSMA-VRP led to increased immunity to PSMA. This finding is consistent with that observed for other VRP vaccines for cancer (16, 17) and highlights the potential for PSMA-VRP to serve as a stand-alone immunization strategy that potentially could be used to periodically restimulate immune responses over the lifetime of the patient. The ability to generate and restimulate long-lived responses without toxicity provides a rationale to explore PSMA-VRP vaccination as a means to prevent relapse of early-stage disease.

The role of $CD8^+$ and $CD4^+$ T lymphocytes in tumor killing has been shown in a large body of preclinical studies (34). Like other VRP vaccines based on Venezuelan equine encephalitis virus (16, 35–37), PSMA-VRP induced Th-1 responses, which are important for activating CTL. Immune splenocytes showed potent CTL activity that specifically lysed $PSMA^+$ cells *ex vivo*. In addition to IFN-γ secretion by $CD8^+$ and $CD4^+$ T cells, the Th-1 bias was reflected in the preferential elicitation by PSMA-VRP of antibody isotypes (mouse IgG2a/IgG2b) that can efficiently mediate effector functions. Fc effector functions have been shown to mediate antitumor effects *in vivo* in preclinical models of other solid tumors (38), and the elicitation of coordinated cellular and humoral responses is a desirable feature of PSMA-VRP.

In head-to-head testing, PSMA-VRP was a more potent immunogen than an adjuvanted PSMA protein vaccine, which did not elicit a significant cellular response. In addition, whereas both PSMA-VRP and PSMA protein elicited robust antibody responses, PSMA-VRP elicited higher levels of antibodies that bound cell surface PSMA. A prior study examined an optimized PSMA DNA plasmid vaccine approach in BALB/c mice (39). In terms of IFN-γ responses, PSMA-VRP compares favorably with the DNA vaccine. In addition, PSMA-VRP elicited robust antibody and CTL responses that were not reported for the DNA vaccine (39).

Our study is the first to explore the epitope specificity of the $CD8^+$ and $CD4^+$ responses induced by an alphavirus vaccine. As determined in our assay system, the PSMA-VRP–induced cellular immune response was focused on a limited number of peptide determinants reactive with $CD8^+$ and $CD4^+$ T lymphocytes, although different peptides were dominant in

BALB/c and C57BL/6 mice. The response in BALB/c mice was directed primarily toward a peptide ($PSMA_{76-90}$, NFTQIPHLAGTEQNF) that may contain both MHC class I and class II epitope(s). In contrast, the $CD8^+$ and $CD4^+$ responses in C57BL/6 animals mapped to separate epitopes: $PSMA_{631-645}$ (SLFSAVKNFTEIASK) and $PSMA_{231-245}$(PADYFAPGVKSYPDG), respectively. For both strains of mice, the peptides responsible for the $CD8^+$ responses were confirmed to contain the respective K^b and K^d MHC class I binding motifs by the SYFPEITHI epitope prediction algorithm (40).[4]

Human $PSMA_{631-645}$ and $PSMA_{231-245}$ peptides are, respectively, 80% and 87% identical with the corresponding murine sequences, and these values bracket the 85% identity shared over the entire protein sequences of human and murine PSMA. $PSMA_{631-645}$ and $PSMA_{231-245}$ are both slightly more homologous (93%) to their murine counterparts than is the protein as a whole (89% homologous). Therefore, the responses observed against the $PSMA_{631-645}$ and $PSMA_{231-245}$ peptides are not due to any obvious degree of interspecies sequence divergence in these regions.

The antigenic determinants of the PSMA-specific IFN-γ responses were determined following stimulation with 15-mer peptide pools in an ELISPOT assay. The peptide responses were similar in magnitude to those observed following stimulation with syngeneic $PSMA^+$ cells; however, it is possible that additional reactivities could be detected using other methods of stimulation and detection. Furthermore, because nonoverlapping antigenic specificities were observed in two in-bred strains of mice, additional diversity could be expected in outbred animals and in humans.

The present report adds to a growing body of data on the preclinical potency of alphavirus-based vaccines for cancer (16, 17, 41). Our prior study with tyrosinase-VRP showed that immune tolerance can be surmounted using Venezuelan equine encephalitis virus VRP encoding either syngeneic or xenogeneic forms of the tumor antigen. In the prior study, higher levels of immunity and tumor protection were observed for VRP encoding mouse rather than human tyrosinase (17), consistent with other studies showing that alphavirus-based DNA and VRP vaccines can overcome immune tolerance to self-antigens and thereby obviate the need for xenoimmunization strategies (16, 41). The potency of alphavirus-based vaccines has been linked to activation of IFN responses and other innate immune mechanisms by double-stranded RNA intermediates formed during the replication cycle (41). In addition, the potency of VRP-based vaccines may reflect their ability to specifically target dendritic cells, Langerhans cells, and other antigen-presenting cells that are critical for priming the immune system (42–45). In the present study, we showed that PSMA-VRP transduction of dendritic cells leads to efficient presentation of PSMA antigen *in vitro*.

The pattern of PSMA expression is not conserved across species. For example, PSMA is not expressed in the mouse prostate or on available mouse prostate cancer cell lines (46), and no relevant PSMA tumor challenge model is available. In addition, no human PSMA transgenic animal model has been developed to examine issues of tolerance to human PSMA. For these reasons and because alphavirus-based vaccines obviate the need for xenoimmunization, as discussed above, we did not evaluate murine PSMA-VRP as a research tool in mice but rather chose to generate and evaluate human PSMA-VRP as a candidate vaccine for human prostate cancer therapy.

PSMA-VRP mediated high-level expression of functional PSMA and strongly elicited long-lived humoral and cellular immune responses in this study. The specificity of the cellular response in mice was mapped to specific peptide determinants using novel and sensitive methods, and these methods are appropriate for immunomonitoring of patients treated with PSMA vaccines. The vaccine was well tolerated in a Good Laboratory Practice toxicology study in male rabbits. We believe that PSMA-VRP provides an attractive new agent for the treatment of progressive prostate cancer and/or the prevention of disease relapse.

[4] http://www.syfpeithi.de/Scripts/MHCServer.dll/EpitopePrediction.htm

References

1. Jemal A, Murray T, Ward E, et al. Cancer statistics, 2005. CA Cancer J Clin 2005;55:10–30.
2. Dagher R, Li N, Abraham S, Rahman A, Sridhara R, Pazdur R. Approval summary: Docetaxel in combination with prednisone for the treatment of androgen-independent hormone-refractory prostate cancer. Clin Cancer Res 2004;10:8147–51.
3. Su SL, Huang IP, Fair WR, Powell CT, Heston WD. Alternatively spliced variants of prostate-specific membrane antigen RNA: ratio of expression as a potential measurement of progression. Cancer Res 1995; 55:1441–3.
4. Israeli RS, Powell CT, Corr JG, Fair WR, Heston WD. Expression of the prostate-specific membrane antigen. Cancer Res 1994;54:1807–11.
5. Sweat SD, Pacelli A, Murphy GP, Bostwick DG. Prostate-specific membrane antigen expression is greatest in prostate adenocarcinoma and lymph node metastases. Urology 1998;52:637–40.
6. Chang SS, Reuter VE, Heston WD, Gaudin PB. Comparison of anti-prostate-specific membrane antigen antibodies and other immunomarkers in metastatic prostate carcinoma. Urology 2001;57:1179–83.
7. Chang SS, Reuter VE, Heston WD, Bander NH, Grauer LS, Gaudin PB. Five different anti-prostate-specific membrane antigen (PSMA) antibodies confirm PSMA expression in tumor-associated neovasculature. Cancer Res 1999;59:3192–8.
8. Chang SS, O'Keefe DS, Bacich DJ, Reuter VE, Heston WD, Gaudin PB. Prostate-specific membrane antigen is produced in tumor-associated neovasculature. Clin Cancer Res 1999;5:2674–81.
9. Chang SS, Reuter VE, Heston WD, Gaudin PB. Metastatic renal cell carcinoma neovasculature expresses prostate-specific membrane antigen. Urology 2001; 57:801–5.
10. Liu H, Moy P, Kim S, et al. Monoclonal antibodies to the extracellular domain of prostate-specific membrane antigen also react with tumor vascular endothelium. Cancer Res 1997;57:3629–34.
11. Silver DA, Pellicer I, Fair WR, Heston WD, Cordon-Cardo C. Prostate-specific membrane antigen expression in normal and malignant human tissues. Clin Cancer Res 1997;3:81–5.
12. Slovin SF. Targeting novel antigens for prostate cancer treatment: focus on prostate-specific membrane antigen. Expert Opin Ther Targets 2005;9:561–70.
13. Ghosh A, Heston WD. Tumor target prostate specific membrane antigen (PSMA) and its regulation in prostate cancer. J Cell Biochem 2004;91:528–39.
14. Lundstrom K. Alphavirus vectors for vaccine production and gene therapy. Expert Rev Vaccines 2003; 2:447–59.
15. Leitner WW, Ying H, Driver DA, Dubensky TW, Restifo NP. Enhancement of tumor-specific immune response with plasmid DNA replicon vectors. Cancer Res 2000;60:51–5.
16. Nelson EL, Prieto D, Alexander TG, et al. Venezuelan equine encephalitis replicon immunization overcomes intrinsic tolerance and elicits effective anti-tumor immunity to the 'self' tumor-associated antigen, neu in a rat mammary tumor model. Breast Cancer Res Treat 2003;82:169–83.
17. Goldberg SM, Bartido SM, Gardner JP, et al. Comparison of two cancer vaccines targeting tyrosinase: plasmid DNA and recombinant alphavirus replicon particles. Clin Cancer Res 2005;11:8114–21.
18. Pushko P, Parker M, Ludwig GV, Davis NL, Johnston RE, Smith JF. Replicon-helper systems from attenuated Venezuelan equine encephalitis virus: expression of heterologous genes *in vitro* and immunization against heterologous pathogens *in vivo*. Virology 1997;239:389–401.
19. Davis NL, Caley IJ, Brown KW, et al. Vaccination of macaques against pathogenic simian

immunodeficiency virus with Venezuelan equine encephalitis virus replicon particles. J Virol 2000;74:371–8.

20. Macpherson I, Stoker M. Polyoma transformation of hamster cell clones—an investigation of genetic factors affecting cell competence. Virology 1962;16:147–51.

21. Rhim JS, Schell K. Cytopathic effects of the parainfluenza virus SV5 in Vero cells. Nature 1967;216:271–2.

22. Brattain MG, Strobel-Stevens J, Fine D, Webb M, Sarrif AM. Establishment of mouse colonic carcinoma cell lines with different metastatic properties. Cancer Res 1980;40:2142–6.

23. Aaronson SA, Todaro GJ. Development of 3T3-like lines from Balb-c mouse embryo cultures: transformation susceptibility to SV40. J Cell Physiol 1968;72:141–8.

24. O'Keefe DS, Uchida A, Bacich DJ, et al. Prostate-specific suicide gene therapy using the prostate-specific membrane antigen promoter and enhancer. Prostate 2000;45:149–57.

25. Tobery TW, Caulfield MJ. Identification of T-cell epitopes using ELISpot and peptide pool arrays. Methods Mol Med 2004;94:121–32.

26. Schulke N, Varlamova OA, Donovan GP, et al. The homodimer of prostate-specific membrane antigen is a functional target for cancer therapy. Proc Natl Acad Sci U S A 2003;100:12590–5.

27. Ma D, Donovan GP, Gardner JP, et al. Fully human anti-PSMA monoclonal antibodies for immunotherapy of metastatic prostate cancer. Cancer Biother Radiopharm 2002;17:484.

28. Pinto JT, Suffoletto BP, Berzin TM, et al. Prostate-specific membrane antigen: a novel folate hydrolase in human prostatic carcinoma cells. Clin Cancer Res 1996;2:1445–51.

29. Ghosh A, Wang X, Klein E, Heston WD. Novel role of prostate-specific membrane antigen in suppressing prostate cancer invasiveness. Cancer Res 2005;65:727–31.

30. Ma D, Hopf C, Malewicz AD, et al. Potent antitumor activity of an auristatin-conjugated, fully human monoclonal antibody to prostate-specific membrane antigen. Clin Cancer Res 2006;12:2591–6.

31. Schroers R, Shen L, Rollins L, et al. Identification of MHC class II-restricted T-cell epitopes in prostate-specific membrane antigen. Clin Cancer Res 2003;9:3260–71.

32. Irvine KR, Chamberlain RS, Shulman EP, Surman DR, Rosenberg SA, Restifo NP. Enhancing efficacy of recombinant anticancer vaccines with prime/boost regimens that use two different vectors. J Natl Cancer Inst 1997;89:1595–601.

33. Overwijk WW, Lee DS, Surman DR, et al. Vaccination with a recombinant vaccinia virus encoding a "self" antigen induces autoimmune vitiligo and tumor cell destruction in mice: requirement for CD4(+) T lymphocytes. Proc Natl Acad Sci U S A 1999;96:2982–7.

34. Yu Z, Restifo NP. Cancer vaccines: progress reveals new complexities. J Clin Invest 2002;110:289–94.

35. Thomas CE, Zhu W, Van Dam CN, Davis NL, Johnston RE, Sparling PF. Vaccination of mice with gonococcal TbpB expressed *in vivo* from Venezuelan equine encephalitis viral replicon particles. Infect Immun 2006;74:1612–20.

36. Gipson CL, Davis NL, Johnston RE, de Silva AM. Evaluation of Venezuelan equine encephalitis (VEE) replicon-based outer surface protein A (OspA) vaccines in a tick challenge mouse model of Lyme disease. Vaccine 2003;21:3875–84.

37. Zhu W, Thomas CE, Chen CJ, et al. Comparison of immune responses to gonococcal PorB delivered as outer membrane vesicles, recombinant protein, or Venezuelan equine encephalitis virus replicon particles. Infect Immun 2005;73:7558–68.

38. Clynes R, Takechi Y, Moroi Y, Houghton A, Ravetch JV. Fc receptors are required in passive and active immunity to melanoma. Proc Natl Acad Sci U S A 1998;95:652–6.

39. Gregor PD, Wolchok JD, Ferrone CR, et al. CTLA-4 blockade in combination with xenogeneic DNA vaccines enhances T-cell responses, tumor immunity and autoimmunity to self antigens in animal and cellular model systems. Vaccine 2004;22:1700–8.

40. Rammensee H, Bachmann J, Emmerich NP, Bachor OA, Stevanovic S. SYFPEITHI: database for MHC ligands and peptide motifs. Immunogenetics 2005;50:213–9.

41. Leitner WW, Hwang LN, deVeer MJ, et al. Alphavirus-based DNA vaccine breaks immunological tolerance by activating innate antiviral pathways. Nat Med 2003;9:33–9.

42. MacDonald GH, Johnston RE. Role of dendritic cell targeting in Venezuelan equine encephalitis virus pathogenesis. J Virol 2000;74:914–22.

43. Moran TP, Collier M, McKinnon KP, Davis NL, Johnston RE, Serody JS. A novel viral system for generating antigen-specific T cells. J Immunol 2005;175:3431–8.

44. Gardner JP, Frolov I, Perri S, et al. Infection of human dendritic cells by a Sindbis virus replicon vector is determined by a single amino acid substitution in the E2 glycoprotein. J Virol 2000;74:11849–57.

45. Shabman RS, Morrison TE, Moore C, et al. Differential induction of type I interferon responses in myeloid dendritic cells by mosquito and mammalian-cell-derived alphaviruses. J Virol 2007;81:237–47.

46. Bacich DJ, Pinto JT, Tong WP, Heston WD. Cloning, expression, genomic localization, and enzymatic activities of the mouse homolog of prostate-specific membrane antigen/NAALADase/folate hydrolase. Mamm Genome 2001;12:117–23.